

## Probing quantum chaos in many-body quantum systems by the induced dissipation

Anna A. Bychek,<sup>1</sup> Pavel S. Muraev,<sup>2</sup> and Andrey R. Kolovsky<sup>1,2</sup>

<sup>1</sup>*Kirensky Institute of Physics, 660036 Krasnoyarsk, Russia*

<sup>2</sup>*Siberian Federal University, 660041 Krasnoyarsk, Russia*



(Received 13 May 2019; published 11 July 2019)

We theoretically analyze the depletion dynamics of an ensemble of cold atoms in a quasi-one-dimensional optical lattice where atoms in one of the lattice sites are subject to decay. Unlike the previous studies of this problem in Labouvie *et al.*, *Phys. Rev. Lett.* **116**, 235302 (2016), we focus on the case where the system is brought to the chaotic regime, which crucially modifies the depletion dynamics as compared to the regular case. It is shown that depletion of the affected site results in gradual depletion of the neighboring sites according to the  $t^{1/3}$  scaling law. We also show that by measuring occupations of the lattice sites one can extract important information on chaotic dynamics of the original conservative system.

DOI: [10.1103/PhysRevA.100.013610](https://doi.org/10.1103/PhysRevA.100.013610)

### I. INTRODUCTION

The term quantum chaos appeared in physics in the late 1980s, although the problem itself can be traced back to 1950s [1] or even to the 1917 paper by Einstein [2]. In a wide sense it means the branch of modern physics dealing with nonintegrable quantum systems and, simultaneously, the variety of phenomena one meets in these systems such as the universal spectral statistics [3–7]. Nowadays the field of quantum chaos consists of several subfields with one of them addressing nonintegrable systems of a large number of identical particles [8–14]. The ultimate goal of these studies is a foundation of the equilibrium and nonequilibrium statistical mechanics by utilizing the universal properties of the energy spectrum and eigenstates of the quantum chaotic systems. For example, it was demonstrated in recent work [14] that, provided the condition of quantum chaos is satisfied, an isolated system of weakly interacting fermions exhibits self-thermalization with meaningful notions of the temperature and chemical potential.

Another development in physics of the last decade is open many-body systems [15–20]. Here the term “open” means that the system of identical particles is coupled to an environment or particle reservoir, and, thus, neither the system energy nor the number of particles is conserved. Generally, there are both the particle gain and loss, as is the case in the cold atom transport in a “lead” connecting two atom reservoirs with different chemical potentials [19,20]. However, in some cases we can have only losses. For example, the authors of the abstract laboratory experiment [21] study dynamics of a Bose-Einstein condensate (BEC) of cold atoms in a quasi-one-dimensional optical lattice where one of the lattice sites is constantly depleted by using a tightly focused electron beam. Merging these two developments one arrives at the problem of *open many-body chaotic systems*, where we may expect some universal dynamics [22].

In the present work we theoretically analyze the system studied in Ref. [21] yet for the principally different initial condition where the BEC of atoms is brought to the edge of the

Brillouine zone. Experimentally this is done by accelerating the lattice or by applying a gradient of the magnetic field for one-half of the Bloch period. As is known, at the zone edge the BEC of repulsively interacting atoms exhibits dynamical or modulation instability that indicates the onset of chaos. We are interested in the depletion dynamics, which is shown to provide important information about chaotic properties of the closed system. Thus, one can use the induced dissipation as a tool for probing quantum chaos in many-body systems.

### II. THE SYSTEM

The system dynamics is governed by the master equation

$$\frac{d\mathcal{R}}{dt} = -i[\widehat{H}, \mathcal{R}] + \widehat{\mathcal{L}}_\gamma(\mathcal{R}) \quad (1)$$

on the density matrix  $\mathcal{R}(t)$  of the ensemble of interacting atoms in a lattice,

$$\widehat{H} = \omega \sum_{l=1}^L \hat{n}_l - \frac{J}{2} \sum_{l=1}^L (\hat{a}_{l+1}^\dagger \hat{a}_l + \text{H.c.}) + \frac{U}{2} \sum_{l=1}^L \hat{n}_l(\hat{n}_l - 1), \quad (2)$$

where the Lindblad operator  $\widehat{\mathcal{L}}_\gamma(\mathcal{R})$ ,

$$\widehat{\mathcal{L}}_\gamma(\mathcal{R}) = -\frac{\gamma}{2}(\hat{a}_l^\dagger \hat{a}_l \mathcal{R} - 2\hat{a}_l \mathcal{R} \hat{a}_l^\dagger + \mathcal{R} \hat{a}_l^\dagger \hat{a}_l), \quad (3)$$

acts only on the single site with the index  $l = L/2$ . In Eqs. (2) and (3)  $\omega$  is the frequency of zero oscillations,  $J$  the hopping matrix elements,  $U$  the microscopic interaction constant, and  $\gamma$  the depletion rate. An additional parameter of the system is the mean occupation number of the lattice sites  $\bar{n}$ . In the experiment [21]  $\bar{n} \approx 700$  atoms,  $J \approx 230$  Hz, and the macroscopic (mean field) interaction constant  $g = U\bar{n} \approx 1400$  Hz.

Below we solve Eq. (1) by using the pseudoclassical approach, which is based on the notion of the truncated Wigner or Husimi functions [23,24]. With respect to cold atoms in optical lattices this approach was used, in particular, to analyze Bloch oscillations of interacting atoms. It was demonstrated

in Ref. [25] that the pseudoclassical approach is capable of reproducing extremely well both results of the exact quantum simulations [25] and the experimental results [26]. Next we briefly review the main statements of this approach (for more details see Refs. [13,27]).

### III. PSEUDOCCLASSICAL APPROACH

In the framework of the pseudoclassical approach the dynamics is described by the distribution function  $f(\mathbf{a}, t)$ , which is a function of time and  $L$  complex variables  $a_l, l = 1, \dots, L$ . Assuming for the moment  $\gamma = 0$  and neglecting the terms  $O(1/\bar{n})$  it satisfies the Liouville equation

$$\frac{\partial f}{\partial t} = \{H, f\}, \quad (4)$$

where  $\{\dots, \dots\}$  denotes the Poisson brackets and  $H$  is the Hamiltonian of the classical Bose-Hubbard model,

$$H = \omega \sum_{l=1}^L a_l^* a_l - \frac{J}{2} \sum_{l=1}^L (a_{l+1}^* a_l + \text{c.c.}) + \frac{g}{2} \sum_{l=1}^L |a_l|^4, \quad (5)$$

where  $g = U\bar{n}$ . [Notice that in Eq. (5) we apply normalization  $\sum_{l=1}^L |a_l|^2 = L$ .] Commonly, one solves Eq. (4) by solving the Hamilton equations of motion,

$$i\dot{a}_l = \frac{\partial H}{\partial a_l^*} = \omega a_l - \frac{J}{2}(a_{l+1} + a_{l-1}) + g|a_l|^2 a_l, \quad (6)$$

and averaging the result over an ensemble of initial conditions with the distribution function  $f(\mathbf{a}, t = 0)$ . For example, for relative occupations of the lattice sites  $n_l(t) = N_l(t)/\bar{n}$  (which are the quantities measured in the laboratory experiment) we have

$$n_l(t) = \text{Tr}[\hat{a}_l^\dagger \hat{a}_l \mathcal{R}(t)]/\bar{n} = \overline{|a_l(t)|^2}, \quad (7)$$

where the overline denotes the ensemble average. Since  $f(\mathbf{a}, t = 0)$  is uniquely determined by the initial many-body wave function of the quantum system (2) we refer to this ensemble of initial conditions as the quantum ensemble. Typically, it is a difficult numerical problem to generate the quantum ensemble. Fortunately, for some important many-body states, such as the BEC or Mott-insulator states, quantum ensembles are known explicitly [13,25].

Next we discuss the classical Bose-Hubbard model (5). Since it can be viewed as the system of  $L$  coupled nonlinear oscillator  $h_l$ ,

$$h_l = \omega I_l + \frac{g}{2} I_l^2, \quad I_l = |a_l|^2, \quad (8)$$

one expects that its dynamics is generally chaotic. As an example, we consider the case  $L = 6$ , which already captures the main properties of larger systems  $L \gg 1$ . The upper panel in Fig. 1 shows the volume of the energy shell as the function of the shell energy for  $g/J = 4$ . (We note, in passing, that the depicted histogram reproduces the density of states of the quantum Bose-Hubbard model [27].) The lower panel in Fig. 1 shows the Lyapunov exponent  $\lambda$  of different trajectories  $\mathbf{a}(t)$  with the initial conditions uniformly distributed over the whole phase space, which is a hypersphere defined by the condition  $\sum_{l=1}^L |a_l|^2 = L$ . Additional vertical lines in Fig. 1(b)

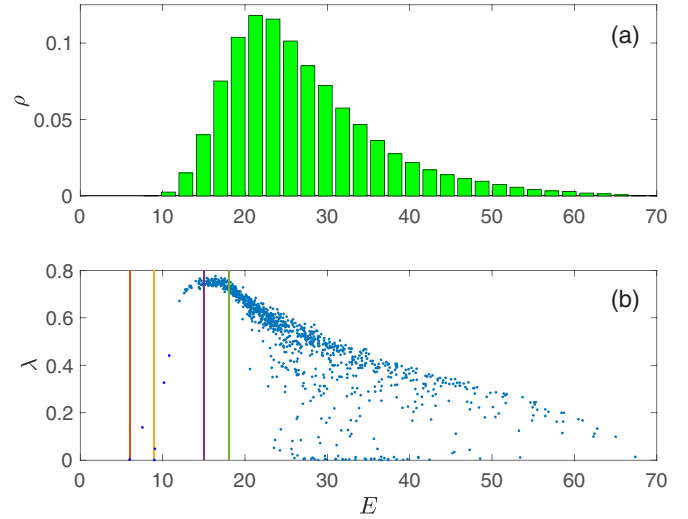


FIG. 1. The classical Bose-Hubbard model. Upper panel: Relative volume of the energy shell as the function of the shell energy  $E$  where energy is measured in units of  $J$ . Lower panel: Lyapunov exponent  $\lambda$  of 1000 trajectories with the initial conditions uniformly distributed over the whole phase space. Vertical lines mark energies of the periodic trajectories (9). Parameters are  $L = 6$  and  $g/J = 4$ .

mark the energies of the nonlinear Bloch waves,

$$a_l(t) = \exp[i\kappa l + iJ \cos(\kappa)t - i\omega t], \quad \kappa = 2\pi k/L, \quad (9)$$

which are stable ( $|\kappa| < \pi/2$ ) or unstable ( $|\kappa| > \pi/2$ ) periodic trajectories of the system. As expected, we find regular trajectories (i.e., vanishing Lyapunov exponent) only for low- and high-energy trajectories while trajectories in the middle of the “spectrum” are chaotic with probability close to unity.

Chaotic dynamics of the system for  $|\kappa| > \pi/2$  implies that the time behavior of fast variables is a random process. In particular, we consider the variable  $\xi(t)$ ,

$$\xi(t) = a_{l+1}(t) + a_{l-1}(t), \quad (10)$$

which is the driving force for the  $l$ th oscillator (8). We found that the autocorrelation function of  $\xi(t)$  is well approximated by the exponential function,

$$\overline{\xi(t)\xi^*(t')} \approx A \exp(-|t - t'|/\tau), \quad (11)$$

$$A = \overline{|a_{l+1}(t)|^2} + \overline{|a_{l-1}(t)|^2} = 2,$$

where the correlation time  $\tau$  is determined by the Lyapunov exponent  $\lambda$ , which, in turn, is determined by the ratio  $g/J$ . Thus, we have some freedom in varying the correlation time  $\tau$  by varying the ratio  $g/J$ .

### IV. DEPLETION DYNAMICS

Assume now that  $\gamma \neq 0$ . In this case Eq. (4) should be complimented by the relaxation term  $\mathcal{L}_\gamma(f)$ . Again neglecting the terms  $O(1/\bar{n})$  we obtain from Eq. (3)

$$\mathcal{L}_\gamma(f) = \frac{\gamma}{2} \left( a \frac{\partial f}{\partial a} + 2f + a^* \frac{\partial f}{\partial a^*} \right), \quad (12)$$

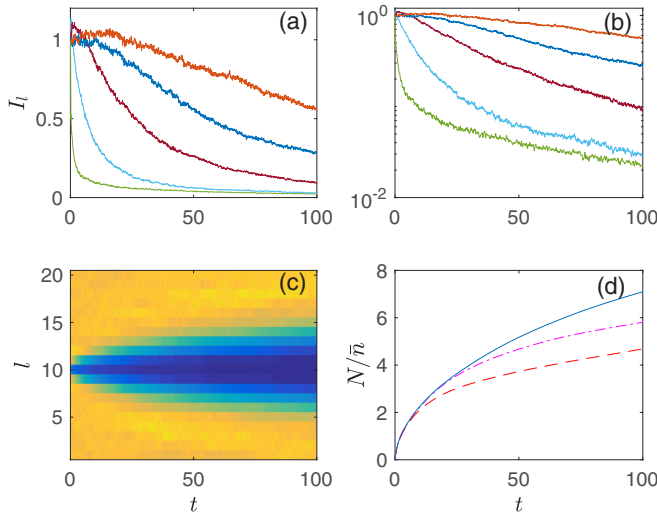


FIG. 2. Occupations of the lattice sites in the course of time where time is measured in units of the tunneling period. Upper panels: Occupations of the lattice sites with  $l = L/2, \dots, L/2 + 4$  (from bottom to top) as functions of time in the linear and logarithmic scales. Lower-left panel: Occupation dynamics as a color map (dark blue = 0, bright yellow = 1). Lower-right panel: Total number of the depleted particles normalized to  $\tilde{n}$  for different positions of the weak link; see text. Parameters are  $L = 20$  (periodic boundary conditions),  $g/J = 4$ , and  $\gamma = 0.1$ . Average over 1000 trajectories.

where we omit subindex  $L/2$  not to overburden the equation (see Appendix A). It is also easy to show that this relaxation term modifies Eq. (6) as

$$i\dot{a}_l = \left( \omega - i\frac{\gamma}{2}\delta_{l,L/2} \right) a_l - \frac{J}{2}(a_{l+1} + a_{l-1}) + g|a_l|^2 a_l. \quad (13)$$

We run Eq. (13) for the initial conditions taken from the quantum ensemble for the BEC of atoms accelerated to the edge of the Brillouin zone. Approximately it corresponds to  $a_l(t=0) \approx (-1)^l$  with tiny fluctuations of the amplitude and phase that are proportional to  $\tilde{n}^{-1/2}$  [25]. However, due to the positive Lyapunov exponent [see Fig. 1(b)] these tiny fluctuations result in completely different trajectories, and, hence, only the average over the ensemble has a physical meaning. This average is depicted in Fig. 2, which shows the occupations of the lattice sites and the total number of depleted atoms,

$$N(t) = \tilde{n} \sum_{l=1}^L [1 - n_l(t)], \quad (14)$$

as the functions of time. Below we quantify the observed occupation dynamics by using some simple approximations.

### A. Short-time dynamics

First, we address the short-time dynamics ( $t < 10$  in Fig. 2) of the central oscillator. Let us for the moment suppress the back action of this oscillator on the other oscillators by changing the hopping between the central well and the neighboring wells with  $l = L/2 \pm 1$  from  $J$  to a small value  $\epsilon J$ ,  $\epsilon \ll 1$ . This reduces the amplitude of the stochastic force proportionally to  $\epsilon$  and, simultaneously, divides the whole

system into the system of interest (the central oscillator) and the reservoir (remaining oscillators). Then the dynamics of the central oscillator is governed by the stochastic equation

$$i\dot{a} = \left( \omega - i\frac{\gamma}{2} \right) a + g|a|^2 a - \frac{\epsilon J}{2} \xi(t), \quad (15)$$

where, as before, we drop the subindex  $l = L/2$ . From Eq. (15) we obtain the equation on the distribution function  $f = f(a, t)$ ,

$$\frac{\partial f}{\partial t} = \{h, f\} + \mathcal{L}_\gamma(f) + D \frac{\partial^2 f}{\partial a \partial a^*}, \quad (16)$$

where the relaxation term  $\mathcal{L}_\gamma(f)$  is defined in Eq. (12) and the diffusion coefficient  $D = \epsilon^2 J^2 \tau / 2$ . (A quantum counterpart of the introduced diffusion term is discussed in Appendix B.) It is easy to prove that the stationary solution of Eq. (16) is given by the two-dimensional Gaussian

$$f(a) = \frac{1}{2\pi\sigma^2} \exp\left(-\frac{|a|^2}{2\sigma^2}\right), \quad (17)$$

where  $\sigma^2 = D/\gamma$ . This determines the relative stationary occupation of the central site as

$$\tilde{n} = \frac{\epsilon^2 J^2 \tau}{2\gamma} \ll 1. \quad (18)$$

Let us now come back to the original system where the artificial parameter  $\epsilon = 1$ . As seen in Figs. 2(a)–2(c), the back action of the central oscillator on the neighboring oscillators results in gradual decay of the latter. A direct consequence of this is that the stationary value  $\tilde{n}$  Eq. (18) becomes quasistationary,

$$\tilde{n}_{L/2}(t) = \frac{J^2 n_{L/2\pm 1}(t) \tau}{2\gamma}, \quad (19)$$

where  $n_{L/2\pm 1}(t)$  is the relative occupation of the nearest sites, and it is implicitly assumed that it is still close to unity. Thus, by measuring the site occupations one can find the correlation time  $\tau$  in Eq. (11).

### B. Long-time dynamics

The above results on the short-time dynamics suffice to qualitatively describe the long-time dynamics of the system. It is a sequence of step-by-step oscillator decay starting from the central oscillator. Furthermore, the decay of every oscillator follows two stages: first, it decays to a quasistationary state characterized by some equilibrium value  $\tilde{n} \ll 1$ , which slowly decreases during the second stage; see Fig. 2(b). [We mention that by a proper rescaling of the time axis the different curves in Figs. 2(a) and 2(b) can be brought above each other.]

The other approach to describe the long-time dynamics is the artificial division of the whole system into the system of interest and the reservoir. In fact, by putting the weak link  $\epsilon J$  far enough from the central site, we reduce the problem to the known problem of an atomic current in the Bose-Hubbard chain, where the first site of the chain is connected to a particle source and the last site to a particle sink (see the recent work [20] and references therein). The dashed, dash-dotted, and solid lines in Fig. 2(d) show the relative number of depleted particles in the cases where the weak links with  $\epsilon = 1/\sqrt{10}$

are located 4, 6, and 10 sites away from the central well, respectively. Notice the asymptotic linear growth of  $N(t)$  in the first two cases, which corresponds to a steady-state regime with the stationary current. According to Ref. [20], the relaxation time to this steady state scales as the chain length to the third power. Inverting this relation, we conclude that the number of depleted wells grow proportionally to  $t^{1/3}$ .

## V. CONCLUSION

We analyzed the depletion dynamics of cold atoms in a quasi-one-dimensional optical lattice where atoms in one of the lattice sites are subject to decay. Experimentally this is done by ionizing the atoms by an electron beam focused on that site [21]. Unlike Ref. [21], in the present work we consider the principally different initial state where the BEC of atoms is brought to the edge of the Brillouin zone. In this case the system is chaotic in the sense of both classical and quantum chaos [13], which crucially modifies the depletion dynamics as compared to the regular case where the BEC is in the ground state (the center of the Brillouin zone). It is predicted that in the chaotic case depletion of the affected site results in a gradual depletion of the neighboring sites, so that the total number of the depleted sites grows  $\sim t^{1/3}$ . We also show that by measuring occupations of the lattice sites one can extract the decay time  $\tau$  for correlation functions of the type  $C(\tau) = \langle \hat{a}_l^\dagger(t) \hat{a}_l(t + \tau) \rangle$  [here  $\hat{a}_l^\dagger(t)$  and  $\hat{a}_l(t)$  are the creation and annihilation operators in the Heisenberg representation]. Keeping in mind that classically the correlation time  $\tau$  is determined by the Lyapunov exponent  $\lambda$  of the classical Bose-Hubbard model, the proposed experimental studies of the depletion dynamics will shed additional light on the long-standing question of the meaning of the classical Lyapunov exponent in the quantum realm.

## ACKNOWLEDGMENTS

This work has been supported through Russian Science Foundation Grant N19-12-00167. The authors are grateful to D. N. Maksimov for stimulating discussions.

## APPENDIX A

In the pseudoclassical approach operators are given by their Wigner-Weyl images. For example, images of the operators  $\tilde{a} = \hat{a}/\sqrt{\bar{n}}$  and  $\tilde{a}^\dagger = \hat{a}^\dagger/\sqrt{\bar{n}}$  (which commutes to the effective Planck constant  $\hbar' = 1/\bar{n}$ ) corresponds to  $a$  and  $a^*$ , respectively. Knowing images of two arbitrary operators  $A = A(a, a^*)$  and  $B = B(a, a^*)$  the image of their product is given by [28]

$$A \star B = A \exp \left[ \frac{\hbar'}{2} \left( \frac{\partial \leftarrow}{\partial a} \frac{\partial \rightarrow}{\partial a^*} - \frac{\partial \leftarrow}{\partial a^*} \frac{\partial \rightarrow}{\partial a} \right) \right] B, \quad (\text{A1})$$

where the the first-order approximation obviously corresponds to

$$A \star B \approx AB + \frac{\hbar'}{2} \left( \frac{\partial A}{\partial a} \frac{\partial B}{\partial a^*} - \frac{\partial A}{\partial a^*} \frac{\partial B}{\partial a} \right). \quad (\text{A2})$$

Applying Eq. (A2) to Eq. (3) we obtain

$$\begin{aligned} \mathcal{L}_\gamma(f) &= -\frac{\gamma}{2\hbar'} (a^* \star a \star f - 2a \star f \star a^* + f \star a^* \star a) \\ &\approx \frac{\gamma}{2} \left( a \frac{\partial f}{\partial a} + 2f + a^* \frac{\partial f}{\partial a^*} \right). \end{aligned} \quad (\text{A3})$$

## APPENDIX B

Let us show that the quantum counterpart of the diffusion term in Eq. (16) is given by the sum of two Lindblad operators,

$$\widehat{\mathcal{D}}(\mathcal{R}) = \widehat{\mathcal{L}}_1(\mathcal{R}) + \widehat{\mathcal{L}}_2(\mathcal{R}), \quad (\text{B1})$$

where

$$\widehat{\mathcal{L}}_1(\mathcal{R}) = -\frac{D\bar{n}}{2} (\hat{a}\hat{a}^\dagger\mathcal{R} - 2\hat{a}^\dagger\mathcal{R}\hat{a} + \mathcal{R}\hat{a}\hat{a}^\dagger), \quad (\text{B2})$$

$$\widehat{\mathcal{L}}_2(\mathcal{R}) = -\frac{D\bar{n}}{2} (\hat{a}^\dagger\hat{a}\mathcal{R} - 2\hat{a}\mathcal{R}\hat{a}^\dagger + \mathcal{R}\hat{a}^\dagger\hat{a}). \quad (\text{B3})$$

Notice that in the first-order approximation the operators (B2) and (B3) have the same form (see Appendix A) but a different sign. Thus,  $\widehat{\mathcal{D}}(\mathcal{R})$  does not vanish only in the second-order approximation. To calculate the second-order Wigner-Weyl image of  $\widehat{\mathcal{D}}(\mathcal{R})$  we rewrite Eq. (B1) as

$$\widehat{\mathcal{D}}(\mathcal{R}) = -\frac{D}{2\hbar'^2} ([\tilde{a}, [\tilde{a}^\dagger, \mathcal{R}]] + [\tilde{a}^\dagger, [\tilde{a}, \mathcal{R}]]). \quad (\text{B4})$$

Using the standard correspondence relation where the commutator corresponds to the Poisson brackets, we obtain from Eq. (B4)

$$\mathcal{D}(f) = -\frac{D}{2} (\{a, \{a^*, f\}\} + \{a^*, \{a, f\}\}) = D \frac{\partial^2 f}{\partial a \partial a^*}. \quad (\text{B5})$$

It is easy to show that the introduced diffusion term leads to unbounded growth of the oscillator action as  $I = Dt$ . This drawback of the model can be eliminated by introducing an effective friction:

$$\mathcal{L}_{\text{eff}}(f) = \frac{D}{2} \left( a \frac{\partial f}{\partial a} + 2f + a^* \frac{\partial f}{\partial a^*} \right). \quad (\text{B6})$$

This additional term naturally appears in the equation on the classical distribution function if we begin with the bosonic relaxation operator of the standard form

$$\begin{aligned} \widehat{\mathcal{L}}(\mathcal{R}) &= -\frac{D}{2} [\bar{n}(\hat{a}\hat{a}^\dagger\mathcal{R} - 2\hat{a}^\dagger\mathcal{R}\hat{a} + \mathcal{R}\hat{a}\hat{a}^\dagger) \\ &\quad + (\bar{n} + 1)(\hat{a}^\dagger\hat{a}\mathcal{R} - 2\hat{a}\mathcal{R}\hat{a}^\dagger + \mathcal{R}\hat{a}^\dagger\hat{a})], \end{aligned} \quad (\text{B7})$$

where the parameter  $D$  is usually referred to as the decay constant. It is understood, however, that the physical meaning of this parameter is the diffusion constant rather than a decay constant. This becomes particularly clear in the case of the induced decay with the rate  $\gamma \gg D$ , where one can neglect the ‘‘internal friction’’ (B6) in comparison with the ‘‘external friction’’ (12). Of course, dividing the relaxation process into diffusion and friction is valid only in the pseudoclassical limit  $\bar{n} \gg 1$ . If  $\bar{n} \sim 1$  one typically speaks about the decoherence and relaxation. With respect to the Bose-Hubbard reservoir with  $\bar{n} \sim 1$  the validity of the master equation with the

relaxation term (B7) was discussed in Ref. [29], with the main conclusion that the necessary and sufficient condition

of its validity is the condition of quantum chaos in the Bose-Hubbard model.

- 
- [1] E. P. Wigner, On the statistical distribution of the widths and spacings of nuclear resonance levels, *Math. Proc. Camb. Philos. Soc.* **47**, 790 (1951).
- [2] A. Einstein, Zum Quantensatz von Sommerfeld und Epstein, *Verh. Dtsch. Phys. Ges.* **19**, 82 (1917). Reprinted in *The Collected Papers of Albert Einstein*, A. Engel translator (Princeton University Press, Princeton, 1997).
- [3] G. M. Zaslavsky, *Stochasticity of Dynamical Systems* (Nauka, Moscow, 1984).
- [4] *Chaos and Quantum Physics*, edited by M. J. Giannoni, A. Voros, and J. Zinn-Justin (North-Holland, Amsterdam, 1991).
- [5] F. Haake, *Quantum Signatures of Chaos* (Springer-Verlag, Berlin, 1992).
- [6] H.-J. Stöckmann, *Quantum Chaos* (Cambridge University Press, Cambridge, 1999).
- [7] L. D'Alessio, Y. Kafri, A. Polkovnikov, and M. Rigol, From quantum chaos and eigenstate thermalization to statistical mechanics and thermodynamics, *Adv. Phys.* **65**, 239 (2016).
- [8] G. Montambaux, D. Poilblanc, J. Bellissard, and C. Sire, Quantum Chaos in Spin-Fermion Models, *Phys. Rev. Lett.* **70**, 497 (1993).
- [9] P. Jacquod and D. L. Shepelyansky, Emergence of Quantum Chaos in Finite Interacting Fermi Systems, *Phys. Rev. Lett.* **79**, 1837 (1997).
- [10] G. P. Berman, F. Borgonovi, F. M. Izrailev, and V. I. Tsifrinovich, Delocalization border and onset of chaos in a model of quantum computation, *Phys. Rev. E* **64**, 056226 (2001).
- [11] A. R. Kolovsky and A. Buchleitner, Quantum chaos in the Bose-Hubbard model, *Europhys. Lett.* **68**, 632 (2004).
- [12] T. A. Elsayed and B. V. Fine, Sensitivity to small perturbations in systems of large quantum spins, *Phys. Scr. T* **165**, 014011 (2015).
- [13] A. R. Kolovsky, Bose-Hubbard Hamiltonian: Quantum chaos approach, *Int. J. Mod. Phys. B* **30**, 1630009 (2016).
- [14] A. R. Kolovsky and D. L. Shepelyansky, Dynamical thermalization in isolated quantum dots and black holes, *Europhys. Lett.* **117**, 10003 (2017).
- [15] D. Witthaut, F. Trimborn, and S. Wimberger, Dissipation Induced Coherence of a Two-Mode Bose-Einstein Condensate, *Phys. Rev. Lett.* **101**, 200402 (2008).
- [16] T. Prosen and B. Žunkovič, Exact solution of Markovian master equations for quadratic Fermi systems: Thermal baths, open XY spin chains and non-equilibrium phase transition, *New J. Phys.* **12**, 025016 (2010).
- [17] P. Barmettler and C. Kollath, Controllable manipulation and detection of local densities and bipartite entanglement in a quantum gas by a dissipative defect, *Phys. Rev. A* **84**, 041606(R) (2011).
- [18] G. Barontini, R. Labouvie, F. Stubenrauch, A. Vogler, V. Guarrera, and H. Ott, Controlling Dynamics of an Open Many-Body Quantum System with Localized Dissipation, *Phys. Rev. Lett.* **110**, 035302 (2013).
- [19] M. Lebrat, P. Grišins, D. Husmann, S. Häusler, L. Corman, T. Giamarchi, J.-Ph. Brantut, and T. Esslinger, Band and Correlated Insulators of Cold Fermions in a Mesoscopic Lattice, *Phys. Rev. X* **8**, 011053 (2018).
- [20] A. R. Kolovsky, Z. Denis, and S. Wimberger, Landauer-Büttiker equation for bosonic carriers, *Phys. Rev. A* **98**, 043623 (2018).
- [21] R. Labouvie, B. Santra, S. Heun, and H. Ott, Bistability in a Driven-Dissipative Superfluid, *Phys. Rev. Lett.* **116**, 235302 (2016).
- [22] A. R. Kolovsky and D. L. Shepelyansky, Evaporative cooling and self-thermalization in an open system of interacting fermions, [arXiv:1902.06929](https://arxiv.org/abs/1902.06929).
- [23] M. J. Steel, M. K. Olsen, L. I. Plimak, P. D. Drummond, S. M. Tan, M. J. Collett, D. F. Walls, and R. Graham, Dynamical quantum noise in trapped Bose-Einstein condensates, *Phys. Rev. A* **58**, 4824 (1998).
- [24] F. Trimborn, D. Witthaut, and H. J. Korsch, Exact number conserving phase-space dynamics of the  $M$ -site Bose-Hubbard model, *Phys. Rev. A* **77**, 043631 (2008).
- [25] A. R. Kolovsky, H.-J. Korsch, and E.-M. Graefe, Bloch oscillations of Bose-Einstein condensates: Quantum counterpart of dynamical instability, *Phys. Rev. A* **80**, 023617 (2009).
- [26] F. Meinert, M. J. Mark, E. Kirilov, K. Lauber, P. Weinmann, M. Gröbner, and H.-C. Nägerl, Interaction-Induced Quantum Phase Revivals and Evidence for the Transition to the Quantum Chaotic Regime in 1D Atomic Bloch Oscillations, *Phys. Rev. Lett.* **112**, 193003 (2014).
- [27] A. R. Kolovsky, Treating many-body quantum systems by means of classical mechanics, in *Emergent Complexity from Nonlinearity, in Physics, Engineering and the Life Sciences*, edited by G. Mantica *et al.*, Springer Proceedings in Physics Vol. 191 (Springer International Publishing AG, 2017), p. 37.
- [28] E. M. Graefe, B. Longstaff, T. Plastow, and R. Schubert, Lindblad dynamics of Gaussian states and their superpositions in the semiclassical limit, *J. Phys. A* **51**, 365203 (2018).
- [29] A. R. Kolovsky, Microscopic models of source and sink for atomtronics, *Phys. Rev. A* **96**, 011601(R) (2017).